Supplementary information

Supplementary Table 1 Primer sequences used for RT-PCR

Supplementary Figure 1. **(a)** Quantitative PCR analysis of autophagy- and mitophagy-related genes in cardiac tissue from Control, HFpEF, and HFpEF+UA mice. **(b)** Immunoblot analysis of mTOR, AKT, AMPKα, and phospho-AMPKα in heart lysates; β-actin was used as a loading control. **(c)** Densitometric quantification of phospho-mTOR/mTOR, phospho-AKT/AKT, and phospho-AMPKα/AMPKα ratios. **(d)** Immunoblot analysis of autophagy initiation–related proteins, including Beclin1, ULK1, p70S6K; β-actin was used as a loading control. **(e)** Densitometric quantification of phospho-Beclin1/Beclin1, phospho-ULK1/ULK1, and phospho-p70S6K/p70S6K ratios. Data are presented as mean ± SEM. Statistical significance was assessed as described in the Methods. *P<0.05, **P<0.01, ***P<0.001, ****P<0.0001.

Supplementary Figure 2. Mitophagy flux and mitochondrial functional assessment in cardiomyocytes. (a) Representative mt-Keima fluorescence images acquired at 445 nm (neutral pH) and 561 nm (acidic pH) from Control, HFpEF, HFpEF+UA, and CCCP-treated positive-control cardiomyocytes. **(b)** Quantification of mt-Keima red/green (561/445 nm) fluorescence ratios. **(c)** Seahorse XF analysis of oxygen consumption rate (OCR) and extracellular acidification rate (ECAR) during mitochondrial stress testing in cardiomyocytes. **(d)** Immunoblot analysis of LC3 A/B and p62/SQSTM1 in cardiomyocytes treated with or without bafilomycin A1 (BafA1); β-actin was used as a loading control. **(e)** Densitometric quantification of p62/β-actin and LC3-II/β-actin ratios in the presence or absence of BafA1. Data are presented as mean ± SEM. Statistical significance was assessed as described in the Methods. *P<0.05, **P<0.01, ***P<0.001.

Supplementary Figure 3. Gut microbiome composition and lipidomic features associated with HFpEF and UA treatment. (a) Bray–Curtis dissimilarity analysis comparing fecal microbial community composition among Control, HFpEF, and HFpEF+UA groups. **(b)** Firmicutes/Bacteroidetes (F/B) ratio calculated from metagenomic profiles. **(c)** Relative abundance of selected ceramide-producing bacterial genera across experimental groups, shown from left to right as Bacteroides, Parabacteroides, Phocaeicola, and Alistipes. **(d)** Z-score heatmap of selected lipidomic species across Control, HFpEF, and HFpEF+UA groups. Data are presented as mean ± SEM. Statistical significance as assessed as described in the Methods. *P<0.05, **P<0.01, ***P<0.001.

Supplementary Figure 4. Fibrosis-associated transcriptional programs and cardiomyocyte state dynamics. (a) ForceAtlas2 (FA1–FA2) embedding of cardiomyocyte nuclei visualizing the mean Z-score expression of a fibrosis-associated gene panel along inferred transcriptional trajectories. **(b)** Relative composition of major cardiomyocyte transcriptional modules across Control, HFpEF, and HFpEF+UA groups. **(c)** Heatmap of significantly altered fibrosis-related genes within fibroblast-enriched transcriptional states, showing per-cell scaled expression across Control, HFpEF, and HFpEF+UA cardiomyocytes. **(d)** Pseudotime dynamics of the fibrosis gene module, displayed as mean Z-score panel scores across Early, Mid, and Late pseudotime phases in Control, HFpEF, and HFpEF+UA cardiomyocytes.

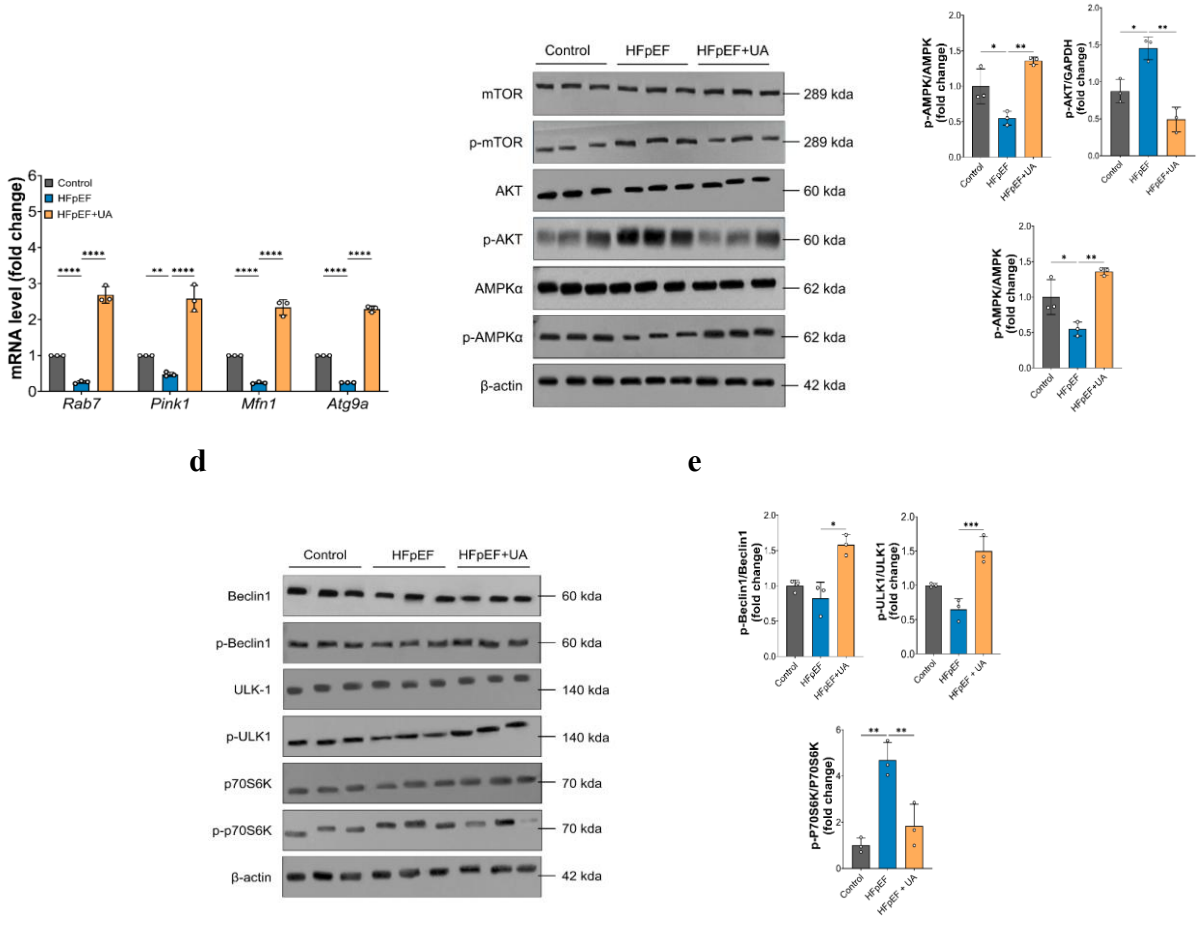

Supplementary Fig. 1

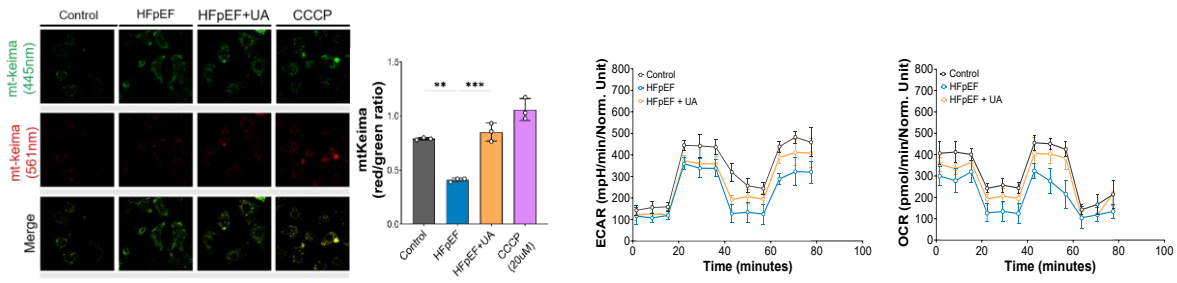

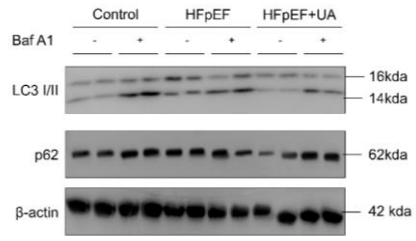

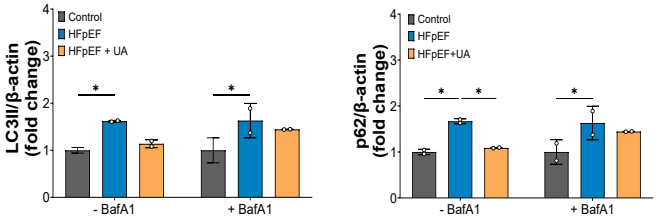

Supplementary Fig. 2

a **b** **c**

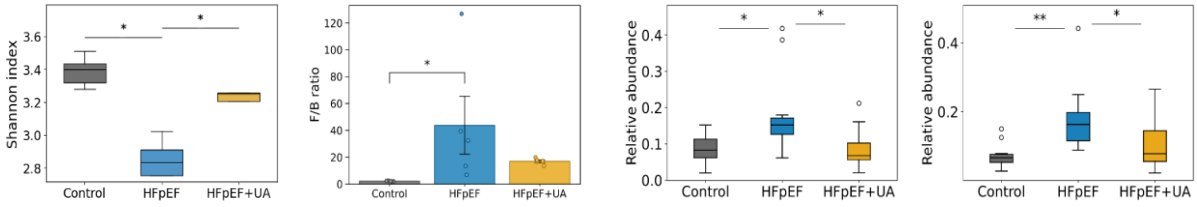

d

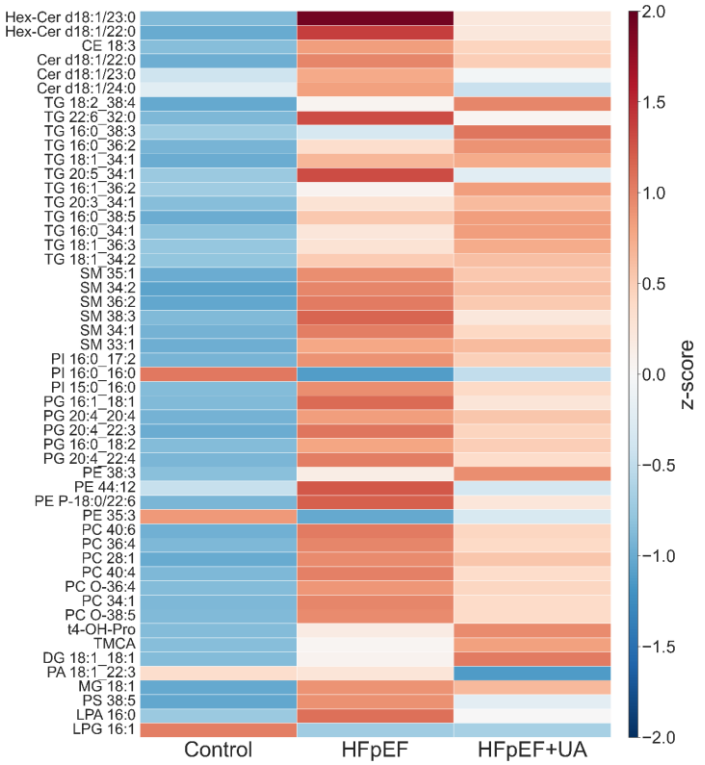

Supplementary Fig. 3

a **b**

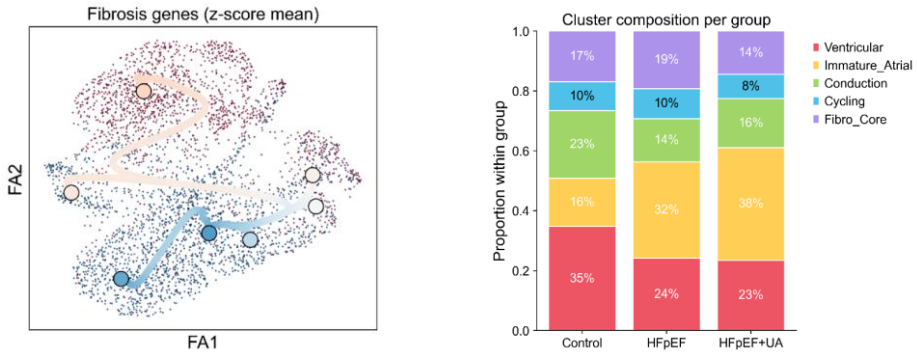

c

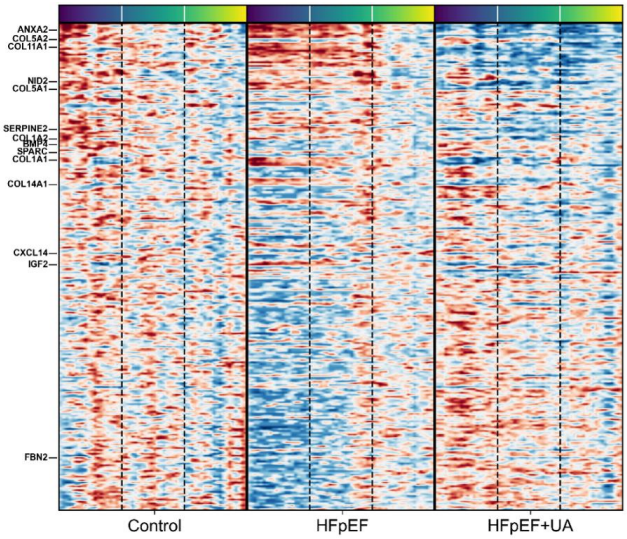

Supplementary Fig.4